physical sciences forum

MDPI

Proceeding Paper

State-Selective Charge Exchange in Collisions of Multiply Charged Ions with H_2 †

Nelson D. Cariatore * and Sebastian Otranto *

Instituto de Física del Sur (IFISUR), Departamento de Física, Universidad Nacional del Sur (UNS), CONICET, Av. L. N. Alem 1253, Bahía Blanca B8000CPB, Argentina

* Correspondence: nelson.cariatore@uns.edu.ar (N.D.C.); sotranto@uns.edu.ar (S.O.)

† Presented at the 1st 1st International Online Conference on Atoms, 29–30 January 2026; Available online: https://sciforum.net/event/IOCAT2026.

Abstract

We report an enhanced Classical Trajectory Monte Carlo (CTMC) approach developed to study state-selective charge exchange in collisions between multiply charged ions and H_2 molecules. The model combines two hydrogenic three-body formulations—originally designed to improve the H(1*s*) radial distribution—within the five-body CTMC framework introduced by Wood and Olson. The new schemes, termed E-CTMC and Z-CTMC, extend the electronic density of the target to larger distances, providing a more accurate representation of the molecular system. Calculations for 2 to 100 keV/u Ne^{9+} and O^{6+} projectiles at low and intermediate impact energies are benchmarked against recent laboratory data and the Multichannel Landau–Zener method. The Z-CTMC approach reproduces the observed energy-dependent shift of the most populated n levels, showing the closest overall agreement with the experiments. Complementary simulations for different projectiles show that discrepancies among the CTMC variants grow with increasing projectile charge and lower impact energies, emphasizing the need for further experimental measurements involving highly charged ions. The present formulation offers a consistent framework for analyzing charge-exchange processes relevant to laboratory and astrophysical plasmas.

Keywords: ion-molecule collisions; charge exchange; state-selective cross sections

1. Introduction

Charge exchange processes involving multiply charged ions and neutral targets play a key role in the modeling of astrophysical environments dominated by high-charge states. In astrophysics, these collisions are primarily responsible for the X-ray and UV emission lines observed in comets, planetary atmospheres, and the solar wind [1,2].

Molecular hydrogen (H_2), being the most abundant molecule in the universe, is a key participant in these interactions. Extensive experimental efforts over several decades have characterized charge exchange in ion-H_2 collisions across a broad range of impact energies [3–30]. These studies have primarily targeted single and double capture cross sections, *n*-resolved state-selective data, and subsequent radiative cascades. To interpret these observations, a wide array of theoretical frameworks has been deployed, ranging from classical treatments like the Bohr–Lindhard [31] and classical-trajectory Monte Carlo (CTMC) [32–35] methods to sophisticated quantum approaches. Notable among the latter are various close-coupling schemes (AOCC, MOCC, SCASCC) [36–39], molecular orbital methods [40,41], the single-particle time-dependent Schrödinger equation (TDSE) [42], and the Multi-Channel Landau–Zener (MCLZ) method [43,44].

Check for updates

Academic Editor: Omar Ariel Fojón

Published: 28 April 2026

Copyright: © 2026 by the authors. Licensee MDPI, Basel, Switzerland. This article is an open access article distributed under the terms and conditions of the Creative Commons Attribution (CC BY) license.

In this work, we use and benchmark the Z-CTMC (Z-expansion Classical Trajectory Monte Carlo) model, designed to improve the classical representation of the H_2 target.

2. Theoretical Method

The standard CTMC treatment of H_2 often relies on a three-body model or a simplified five-body model. In our approach, we adopt the five-body framework proposed by Wood and Olson, which explicitly considers the two protons of the H_2 molecule, two active electrons, and the incoming projectile. In this configuration, each electron interacts exclusively with its corresponding parent nucleus at the start of the simulation.

However, a well-known limitation of the classical microcanonical distribution is its inability to accurately reproduce the quantum-mechanical radial distribution of the $H(1s)$ state. As shown in Figure 1, the electronic cloud has a specific spatial extension that determines the probability of capture at different impact parameters.

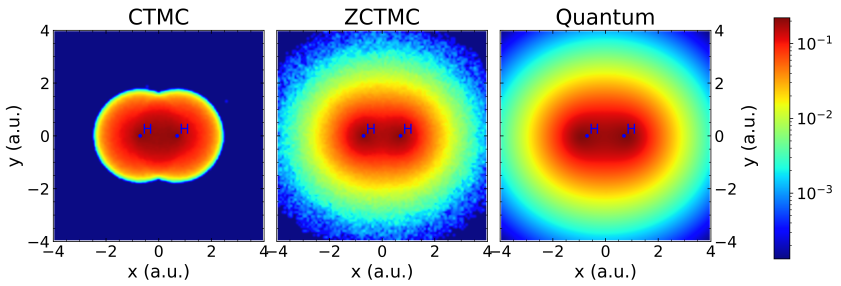


Figure 1. Representation of logarithmic electron densities in the xy molecular plane for H_2.

In the Z-CTMC framework [45,46], the initial state is represented by a weighted superposition of microcanonical ensembles spanning a distribution of nuclear charges (Z). This approach effectively addresses the artificial spatial truncation inherent in standard $Z = 1$ models by populating classically forbidden regions, thus providing a classical analog to the quantum-mechanical tail of the target wavefunction. Regarding the H_2 target, the molecule is modeled as two hydrogen atoms bound by a Morse potential, which maintains the nuclei in their fundamental vibrational state. To ensure physical consistency, the model is constrained to preserve the experimental ionization energy, thereby reconciling the classical dynamical evolution with the correct quantum energetic threshold of the system.

During the dynamical evolution, the electronic energy relative to its parent nucleus is continuously monitored. If an electron reaches the continuum, all interactions previously omitted from the Hamiltonian are progressively reintroduced via a switching function. This mechanism enables the model to intrinsically differentiate between events where the residual molecular ion remains bound as H_2^+ or undergoes fragmentation—a distinction that is crucial for a meaningful comparison with experimental data.

Furthermore, unlike the E-CTMC approach, the Z-CTMC model ensures the correct deposition of ionization energy, resulting in an improved description of state-selective capture. This is particularly relevant since the most probable capture state n follows the scaling law $n \approx \sqrt{13.6/IP}\, q^{3/4}$, where IP is the ionization energy and q is the projectile charge. Indeed, recent benchmarks comparing the Z-CTMC and E-CTMC methods for state-selective electron capture in atomic hydrogen have shown that the Z-CTMC methodology yields superior agreement with advanced quantum-mechanical frameworks, such as two-center atomic orbital close-coupling (TC-AOCC) and two-center wave-packet convergent close-coupling (WP-CCC) [47].

https://doi.org/10.3390/psf2026013004

3. Results and Discussion

3.1. The H_2 Target Description

An analysis of the H_2 molecular representation is provided in Figure 2, which compares the electronic density probability along the internuclear axis. This figure contrasts the quantum mechanical density, obtained from the Schrödinger equation solution [48], with three classical frameworks: the pioneering multicenter CTMC model proposed by Meng et al. [33], based on independent microcanonical ensembles; the energy-adjusted E-CTMC, which introduces an energy distribution in order to correct the radial distribution of the bound electron [49,50] to the initial state; and the present Z-CTMC approach.

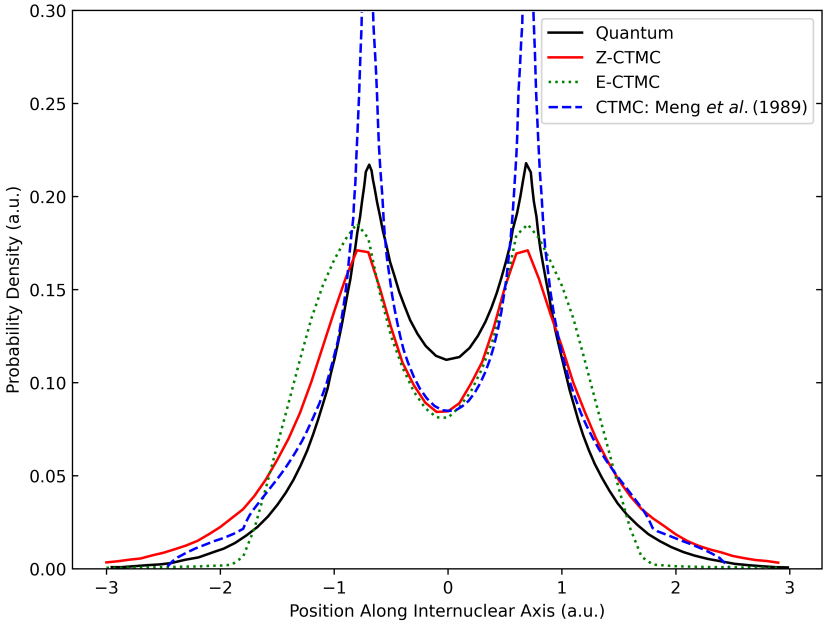


Figure 2. Electronic probability density of the H_2 orbital, as a function of the internuclear distance. Z-CTMC and E-CTMC are compared with Quantum and CTMC model proposed by Meng et al. [33].

Figures 1 and 2 contrast the electronic density of H_2 across various classical frameworks against a quantum-mechanical benchmark. While all models correctly identify the nuclear peaks near ± 0.7 a.u., their spatial distributions vary significantly. The standard CTMC model [33] exhibits highly localized peaks and a sharp boundary, failing to represent either the bonding region or the quantum tail due to its rigid spatial truncation, observed in Figure 1. The E-CTMC model provides an intermediate improvement at the internuclear center; however, its distribution tail displays an anomalous change in slope, becoming broader than both the quantum and other classical theories. In contrast, the present Z-CTMC model provides an optimal balance, yielding smooth, finite peaks and an electron population tail whose slope accurately mirrors quantum theory. By superimposing multiple Z-values to effectively soften classical turning points, the Z-CTMC populates classically forbidden regions and mimics the characteristic exponential decay of the wavefunction. This is evidenced by the diffuse, cloud-like distributions in Figure 1.

3.2. $O^{6+} + H_2$

The Q-value distributions for n-state-selective nondissociative single capture (SEC) in $O^{6+} + H_2$ collisions are shown in Figure 3 for several impact energies. Here, Q represents the change in electronic binding energy throughout the process. These theoretical predictions are benchmarked against recent COLTRIMS measurements [29] to assess the model's accuracy. The Z-CTMC model (solid red line) shows remarkable agreement with the exper-

imental COLTRIMS data. Specifically, at lower energies, Z-CTMC correctly identifies the dominance of the $n = 4$ state and captures the width of the distribution more accurately than standard models.

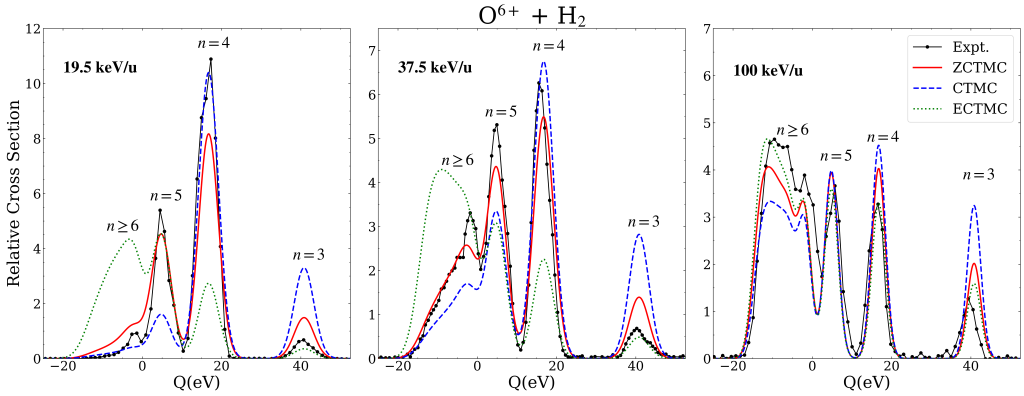


Figure 3. SEC Q spectra for O^{6+} collisions on H_2. Theoretical predictions from CTMC models are contrasted with experimental data.

3.3. $Ne^{9+} + H_2$

An analogous analysis for Ne^{9+} projectiles is presented in Figure 4, where results from the CTMC models are contrasted with recent COLTRIMS measurements and MCLZ calculations [30]. Due to the high charge state of the projectile, electron capture predominantly populates higher principal quantum shells, specifically $n = 5$ and $n = 6$. Notably, the Z-CTMC model accurately reproduces the energy-dependent shift in the Q-value peaks observed experimentally.

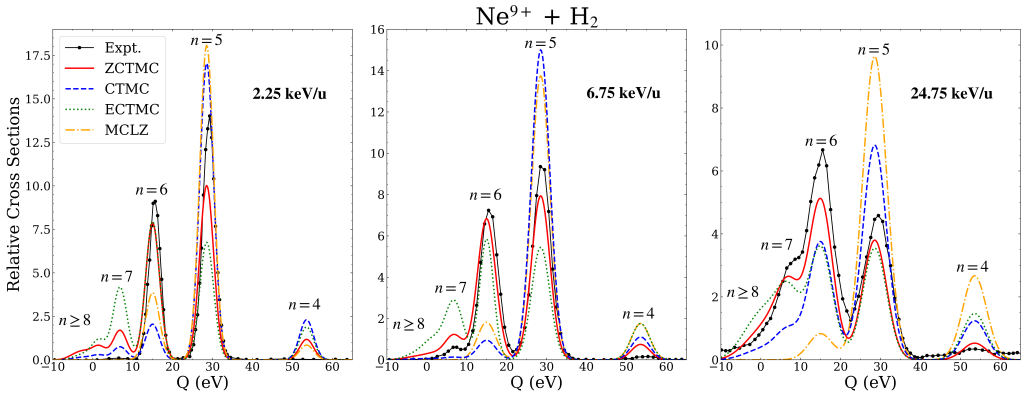


Figure 4. Relative cross sections (Q spectra) for $Ne^{9+} + H_2$ systems highlighting the n-state selectivity.

3.4. Total Cross Sections

Figure 5 displays the total single-electron capture (SEC) cross sections for O^{6+} projectiles. The Z-CTMC calculations are benchmarked against available experimental data [8,16,21,25,28] and the MCLZ results of Gao et al. [39]. These results demonstrate that the Z-CTMC model provides a reliable description of the transition into the low-energy regime (<5 keV/amu), consistently remaining within the experimental uncertainties throughout the investigated energy range.

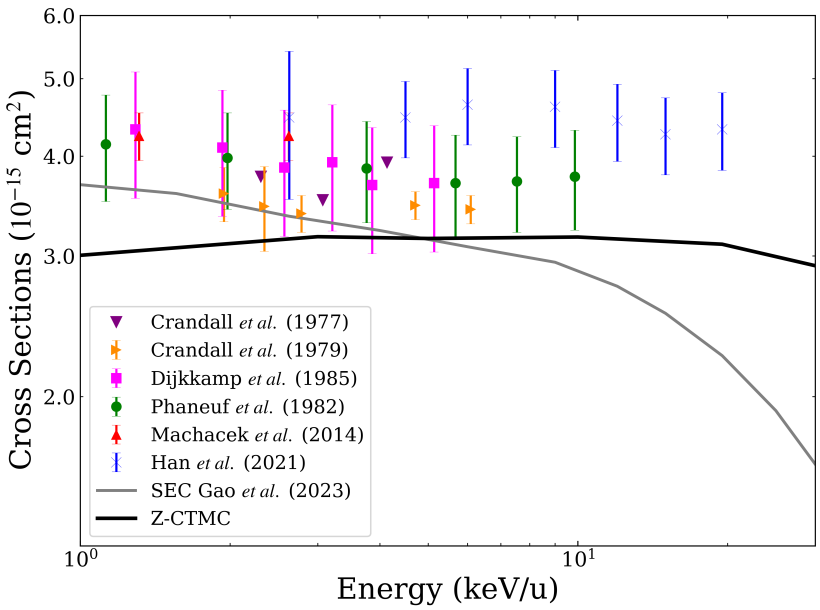


Figure 5. Total single-electron capture cross sections for the $O^{6+} + H_2$ system as a function of impact energy. Z-CTMC model is compared with the theoretical MCLZ model [39] and with experimental measurements from Crandall et al. [8,9], Dijkkamp et al. [21], Phaneuf et al. [16], Machacek et al. [25], and Han et al. [28].

4. Conclusions

In summary, the implementation of the Z-CTMC model represents a significant advancement in the classical description of the H_2 molecular target. The Z-CTMC framework provides an optimal balance by mirroring the exponential 'tail' of the quantum-mechanical wavefunction.This refined initial-state representation is fundamental to the accurate description of collision dynamics. The superior spatial distribution of the Z-CTMC model directly translates into improved agreement with experimental Q-value distributions for highly charged ions like O^{6+} and Ne^{9+}, successfully capturing energy-dependent peak shifts. These results confirm that a physically grounded classical representation of the molecular density is essential for predicting state-selective processes in highly ionized environments.

Author Contributions: N.D.C. and S.O. developed the routines of the code. N.D.C. performed the numerical calculations and contributed to the final manuscript. S.O. contributed to the final manuscript and supervised the project. All authors have read and agreed to the published version of the manuscript.

Funding: This research was funded by Secretaría General de Ciencia y Tecnología, Universidad Nacional del Sur, Argentina, grant number PGI/F084.

Institutional Review Board Statement: Not applicable.

Informed Consent Statement: Not applicable.

Data Availability Statement: The data that support the findings of this study are available from the corresponding authors upon reasonable request.

Conflicts of Interest: The authors declare no conflicts of interest.

References

1. Lisse, C.M.; Dennerl, K.; Englhauser, J.; Harden, M.; Marshall, F.E.; Mumma, M.J.; Petre, R.; Pye, J.P.; Ricketts, M.J.; Schmitt, J.; et al. Discovery of X-ray and Extreme Ultraviolet Emission from Comet C/Hyakutake 1996 B2. *Science* **1996**, *274*, 205–209. [CrossRef]

2. Cravens, T.E. Comet Hyakutake x-ray source: Charge transfer of solar wind heavy ions. *Geophys. Res. Lett.* **1997**, *24*, 105–108. [CrossRef]
3. Barnett, C.F.; Stier, P.M. Charge Exchange Cross Sections for Helium Ions in Gases. *Phys. Rev.* **1958**, *109*, 385–390. [CrossRef]
4. De Heer, F.; Schutten, J.; Moustafa, H. Ionization and electron capture cross sections for protons incident on noble and diatomic gases between 10 and 140 keV. *Physica* **1966**, *32*, 1766–1792. [CrossRef]
5. Baragiola, R.; Nemirovsky, I. Cross sections for single and double electron capture from He^{++} on hydrogen, neon and argon. *Nucl. Instrum. Methods* **1973**, *110*, 511–513. [CrossRef]
6. Shah, M.B.; Gilbody, H.B. Formation of He^{+}(2S) metastable ions in passage of 10-60 keV $^{3}He^{2+}$ ions through gases. *J. Phys. B At. Mol. Phys.* **1974**, *7*, 256. [CrossRef]
7. Bayfield, J.E.; Khayrallah, G.A. Electron transfer in keV-energy $^{4}He^{++}$ atomic collisions. I. Single and double electron transfer with He, Ar, H_2, and N_2. *Phys. Rev. A* **1975**, *11*, 920–929. [CrossRef]
8. Crandall, D.H.; Mallory, M.L.; Kocher, D.C. Charge exchange between multicharged ions of C, N, and O and molecular hydrogen. *Phys. Rev. A* **1977**, *15*, 61–69. [CrossRef]
9. Crandall, D.H.; Phaneuf, R.A.; Meyer, F.W. Electron capture by slow multicharged ions in atomic and molecular hydrogen. *Phys. Rev. A* **1979**, *19*, 504–514. [CrossRef]
10. Phaneuf, R.A.; Meyer, F.W.; McKnight, R.H. Single-electron capture by multiply charged ions of carbon, nitrogen, and oxygen in atomic and molecular hydrogen. *Phys. Rev. A* **1978**, *17*, 534–545. [CrossRef]
11. Kim, H.J.; Phaneuf, R.A.; Meyer, F.W.; Stelson, P.H. Single electron capture by multiply charged ^{28}Si ions in atomic and molecular hydrogen. *Phys. Rev. A* **1978**, *17*, 854–858. [CrossRef]
12. Shah, M.B.; Goffe, T.V.; Gilbody, H.B. Electron capture and loss by fast lithium ions in H and H_2. *J. Phys. B At. Mol. Phys.* **1978**, *11*, L233. [CrossRef]
13. Meyer, F.W.; Phaneuf, R.A.; Kim, H.J.; Hvelplund, P.; Stelson, P.H. Single-electron-capture cross sections for multiply charged O, Fe, Mo, Ta, W, and Au ions incident on H and H_2 at intermediate velocities. *Phys. Rev. A* **1979**, *19*, 515–525. [CrossRef]
14. Goffe, T.V.; Shah, M.B.; Gilbody, H.B. One-electron capture and loss by fast multiply charged boron and carbon ions in H and H_2. *J. Phys. B At. Mol. Phys.* **1979**, *12*, 3763. [CrossRef]
15. Berkner, K.H.; Graham, W.G.; Pyle, R.V.; Schlachter, A.S.; Stearns, J.W. Electron-capture, electron-loss, and impact-ionization cross sections for 103- to 3400-keV/amu multicharged iron ions colliding with molecular hydrogen. *Phys. Rev. A* **1981**, *23*, 2891–2904. [CrossRef]
16. Phaneuf, R.A.; Alvarez, I.; Meyer, F.W.; Crandall, D.H. Electron capture in low-energy collisions of C^{q+} and O^{q+} with H and H_2. *Phys. Rev. A* **1982**, *26*, 1892–1906. [CrossRef]
17. Rudd, M.E.; DuBois, R.D.; Toburen, L.H.; Ratcliffe, C.A.; Goffe, T.V. Cross sections for ionization of gases by 5-4000-keV protons and for electron capture by 5-150-keV protons. *Phys. Rev. A* **1983**, *28*, 3244–3257. [CrossRef]
18. Panov, M.N.; Basalaev, A.A.; Lozhkin, K.O. Interaction of Fully Stripped, Hydrogenlike and Heliumlike C, N, O, Ne and Ar Ions with H and He Atoms and H_2 Molecules. *Phys. Scr.* **1983**, *1983*, 124. [CrossRef]
19. Graham, W.G.; Berkner, K.H.; Pyle, R.V.; Schlachter, A.S.; Stearns, J.W.; Tanis, J.A. Charge-transfer cross sections for multiply charged ions colliding with gaseous targets at energies from 310 keV/amu to 8.5 MeV/amu. *Phys. Rev. A* **1984**, *30*, 722–728. [CrossRef]
20. Rudd, M.E.; Goffe, T.V.; Itoh, A. Ionization cross sections for 10–300-keV/u and electron-capture cross sections for 5–150-keV/u $^{3}He^{2+}$ ions in gases. *Phys. Rev. A* **1985**, *32*, 2128–2133. [CrossRef] [PubMed]
21. Dijkkamp, D.; Gordeev, Y.S.; Brazuk, A.; Drentje, A.G.; de Heer, F.J. Selective single-electron capture into (n, l) subshells in slow collisions of C^{6+}, N^{6+}, O^{6+} and Ne^{6+} with He, H_2 and Ar. *J. Phys. B At. Mol. Phys.* **1985**, *18*, 737. [CrossRef]
22. Greenwood, J.B.; Williams, I.D.; Smith, S.J.; Chutjian, A. Experimental investigation of the processes determining x-ray emission intensities from charge-exchange collisions. *Phys. Rev. A* **2001**, *63*, 062707. [CrossRef]
23. Mawhorter, R.J.; Greenwood, J.B.; Chutjian, A.; Haley, T.; Mitescu, C.D.; Simcic, J. Measurement of absolute charge-exchange cross sections for He^{2+} collisions with He and H_2. *Phys. Rev. A* **2011**, *84*, 052714. [CrossRef]
24. Alessi, M.; Cariatore, N.D.; Focke, P.; Otranto, S. State-selective electron capture in He^{+} + H_2 collisions at intermediate impact energies. *Phys. Rev. A* **2012**, *85*, 042704. [CrossRef]
25. Machacek, J.R.; Mahapatra, D.P.; Schultz, D.R.; Ralchenko, Y.; Chutjian, A.; Simcic, J.; Mawhorter, R.J. Measurement and calculation of absolute single- and double-charge-exchange cross sections for O^{6+} ions at 1.17 and 2.33 keV/u impacting He and H_2. *Phys. Rev. A* **2014**, *90*, 052708. [CrossRef]
26. Fogle, M.; Wulf, D.; Morgan, K.; McCammon, D.; Seely, D.G.; Draganić, I.N.; Havener, C.C. X-ray-emission measurements following charge exchange between C^{6+} and H_2. *Phys. Rev. A* **2014**, *89*, 042705. [CrossRef]
27. Kröger, F.M.; Weber, G.; Herdrich, M.O.; Glorius, J.; Langer, C.; Slavkovská, Z.; Bott, L.; Brandau, C.; Brückner, B.; Blaum, K.; et al. Electron capture of Xe^{54+} in collisions with H_2 molecules in the energy range between 5.5 and 30.9 MeV/u. *Phys. Rev. A* **2020**, *102*, 042825. [CrossRef]

28. Han, J.; Wei, L.; Wang, B.; Ren, B.; Yu, W.; Zhang, Y.; Zou, Y.; Chen, L.; Xiao, J.; Wei, B. Measurement of Absolute Single and Double Electron Capture Cross Sections for O^{6+} Ion Collisions with CO_2, CH_4, H_2, and N_2. *Astrophys. J. Suppl. Ser.* **2021**, *253*, 6. [CrossRef]
29. Xu, J.W.; Xu, C.X.; Zhang, R.T.; Zhu, X.L.; Feng, W.T.; Gu, L.; Liang, G.Y.; Guo, D.L.; Gao, Y.; Zhao, D.M.; et al. Measurement of n-resolved State-selective Charge Exchange in $Ne^{(8,9)+}$ Collision with He and H_2. *Astrophys. J. Suppl. Ser.* **2021**, *253*, 13. [CrossRef]
30. Cao, T.; Meng, T.; Gao, Y.; Zhang, S.F.; Zhang, R.T.; Yan, S.; Zhu, X.L.; Wang, J.; Ma, P.; Ren, B.; et al. State-selective Charge Exchange in 19.5–100 keV amu-1 O^{6+} Collision with He and H_2. *Astrophys. J. Suppl. Ser.* **2023**, *266*, 20. [CrossRef]
31. Knudsen, H.; Haugen, H.K.; Hvelplund, P. Single-electron capture by highly charged ions colliding with atomic and molecular hydrogen. *Phys. Rev. A* **1981**, *24*, 2287–2290. [CrossRef]
32. Olson, R.E.; Salop, A.; Phaneuf, R.A.; Meyer, F.W. Electron loss by atomic and molecular hydrogen in collisions with $^3He^{++}$ and $^4He^+$. *Phys. Rev. A* **1977**, *16*, 1867–1872. [CrossRef]
33. Meng, L.; Reinhold, C.O.; Olson, R.E. Electron removal from molecular hydrogen by fully stripped ions at intermediate energies. *Phys. Rev. A* **1989**, *40*, 3637–3645. [CrossRef]
34. Kerby, G.W.; Gealy, M.W.; Hsu, Y.Y.; Rudd, M.E.; Schultz, D.R.; Reinhold, C.O. Energy and angular distributions of electrons from ion impact on atomic and molecular hydrogen. II. 20–114-keV H^+ + H. *Phys. Rev. A* **1995**, *51*, 2256–2264. [CrossRef] [PubMed]
35. Wood, C.J.; Olson, R.E. Double electron removal and fragmentation model of the H_2 molecule by highly charged ions. *Phys. Rev. A* **1999**, *59*, 1317–1328. [CrossRef]
36. Hedrick, A.F.; Moran, T.F.; McCann, K.J.; Flannery, M.R. Charge transfer cross sections in argon ion–diatomic molecule collisions. *J. Chem. Phys.* **1977**, *66*, 24–31. [CrossRef]
37. Shingal, R.; Lin, C.D. Orientation-dependent atomic model for electron transfer in ion-molecule collisions: Applications to H^+ + H_2 and He^{2+} + H_2. *Phys. Rev. A* **1989**, *40*, 1302–1309. [CrossRef] [PubMed]
38. Kumar, A.; Saha, B.C. State-selective charge transfer in slow collisions of partially stripped He-like ions with H_2. *Phys. Rev. A* **1999**, *59*, 1273–1283. [CrossRef]
39. Gao, J.W.; Qi, Y.Y.; Wu, Y.; Wang, J.G. Single- and Double-electron Capture Cross Sections for O^{6+} Ion in Collisions with H_2 Molecules. *Astrophys. J.* **2023**, *944*, 167. [CrossRef]
40. Gargaud, M.; McCarroll, R. Charge transfer in low-energy collisions of N^{3+}, C^{4+} and N^{5+} with H and H_2. *J. Phys. B At. Mol. Phys.* **1985**, *18*, 463. [CrossRef]
41. Kimura, M.; Chapman, S.; Lane, N.F. Electron capture in Ar^+ + H_2 collisions in the keV energy regime. *Phys. Rev. A* **1986**, *33*, 1619–1625. [CrossRef]
42. Leung, A.C.K.; Kirchner, T. Analysis of x-ray emission spectra in charge-exchange collisions of C^{6+} with He and H_2. *Phys. Rev. A* **2016**, *93*, 052710. [CrossRef]
43. Mullen, P.D.; Cumbee, R.S.; Lyons, D.; Stancil, P.C. Charge exchange-induced X-ray emission of Fe xxv and Fe xxvi via a Streamlined Model. *Astrophys. J. Suppl. Ser.* **2016**, *224*, 31. [CrossRef]
44. Cumbee, R.S.; Mullen, P.D.; Lyons, D.; Shelton, R.L.; Fogle, M.; Schultz, D.R.; Stancil, P.C. Charge Exchange X-Ray Emission due to Highly Charged Ion Collisions with H, He, and H_2: Line Ratios for Heliospheric and Interstellar Applications. *Astrophys. J.* **2017**, *852*, 7. [CrossRef]
45. Cariatore, N.D.; Otranto, S.; Olson, R.E. Classical description of H(1s) and H(n=2) for cross-section calculations relevant to charge-exchange diagnostics. *Phys. Rev. A* **2015**, *91*, 042709. [CrossRef]
46. Cariatore, N.D.; Otranto, S.; Olson, R.E. Reply to "Comment on 'Classical description of $H(1s)$ and $H^*(n=2)$ for cross-section calculations relevant to charge-exchange diagnostics'". *Phys. Rev. A* **2016**, *93*, 066702. [CrossRef]
47. Cariatore, N.D.; Bachi, N.; Acebal, E.; Otranto, S. State-selective electron capture in bare Ne and Ar collisions with H(1s): A critical analysis of classical trajectory methods of relevance for charge-exchange recombination spectroscopy. *Plasma Phys. Control. Fusion* **2025**, *67*, 055003. [CrossRef]
48. Wang, S.C. The Problem of the Normal Hydrogen Molecule in the New Quantum Mechanics. *Phys. Rev.* **1928**, *31*, 579–586. [CrossRef]
49. Hardie, D.J.W.; Olson, R.E. Charge transfer and ionisation processes involving multiply charged ions in collision with atomic hydrogen. *J. Phys. B At. Mol. Phys.* **1983**, *16*, 1983. [CrossRef]
50. Cohen, J.S. Classical phase-space distributions for atomic hydrogen collisions. *J. Phys. B At. Mol. Phys.* **1985**, *18*, 1759. [CrossRef]

Disclaimer/Publisher's Note: The statements, opinions and data contained in all publications are solely those of the individual author(s) and contributor(s) and not of MDPI and/or the editor(s). MDPI and/or the editor(s) disclaim responsibility for any injury to people or property resulting from any ideas, methods, instructions or products referred to in the content.